String Instruments: Paper ICA2016-821

Improved frequency-dependent damping for time domain modelling of linear string vibration

Charlotte Desvages[a], Stefan Bilbao[b], Michele Ducceschi[c]

[a] Acoustics and Audio Group, University of Edinburgh, United Kingdom,
charlotte.desvages@ed.ac.uk
[b] Acoustics and Audio Group, University of Edinburgh, United Kingdom, s.bilbao@ed.ac.uk
[c] Acoustics and Audio Group, University of Edinburgh, United Kingdom,
michele.ducceschi@ed.ac.uk

Abstract

Lossy linear stiff string vibration plays an important role in musical acoustics. Experimental studies have demonstrated the complex dependence of decay time with frequency, confirmed by detailed modelling of dissipated power in linear strings. Losses at a particular frequency can be expressed as a function of the physical parameters defining the system; damping due to air viscosity is predominant at low frequencies, whereas internal friction prevails in the higher frequency range. Such a frequency domain characterisation is clearly well-suited to simulation methods based on, e.g., modal decompositions, for experimental comparison or sound synthesis. However, more general string models might include features difficult to realise with such models, in particular nonlinear effects. In this case, it is useful to approach modelling directly in the space-time domain. This work is concerned with the translation of the frequency domain damping characteristics to a space-time domain framework, leading, ultimately, to a coupled system of partial differential equations. Such a system can be used as a starting point for a time-stepping algorithm; an important constraint to ensure numerical stability is then that of passivity, or dissipativity. Candidate loss terms are characterised in terms of positive real functions, as a starting point for optimisation procedures. Simulation results are presented for a variety of linear strings.

Keywords: physical modelling, sound synthesis, finite difference, passive systems

Improved frequency-dependent damping for time domain modelling of linear string vibration

1   Introduction

Realistic sound synthesis for musical strings has employed physical modelling methods, in the frequency and time domain. Linear models, in particular, can describe the behaviour of most musical strings to a reasonable extent [1]. Previous string models have used modal decomposition [2], travelling wave solutions [3], or direct resolution of a discretised wave equation [4, 5, 6].

While the undamped stiff string problem is defined by a set of easily measurable physical parameters, realistic modelling must account for the frequency dependence of the loss profile. A pioneering study by Cuesta and Valette [7] provided a theoretical expression for the quality factor of harpsichord string modes as a function of frequency, closely fitting experimental measurements. This frequency-domain description of damping in linear strings was straightforwardly implemented in a modal simulation of guitar strings [8]. More damping models have been investigated in other structures [9, 10].

However, deriving a suitable loss profile for time domain models is far from straightforward. In particular, models relying on a discretisation of a space-time domain system/system of partial differential equations [4, 5, 6], arguably the best suited to include more complex, possibly nonlinear phenomena and interactions, have often employed simplified descriptions of damping processes. In this work, we propose a passive system of partial differential equations describing the oscillations of a damped, stiff string. Suitable approximations are made in the transform domain, leading to a tractable optimisation problem, fitting coefficients to match the theoretical loss profile of the string defined by its physical parameters.

Section 2 presents a basic model for linear, undamped stiff string vibration, in the space-time framework. Section 3 introduces the theoretical loss profile for a set of physical parameters defining a particular string. Section 4 introduces losses in the space-time domain system, by the means of positive real functions of the Laplace variable. Section 5 links the proposed model to the theoretical profile, by means of approximations and optimisation. Finally, Section 6 briefly presents preliminary simulation results, obtained by direct resolution of the discretised time-domain system, and Section 7 discusses possible extensions to this work.

2   A space-time domain model of the stiff string

2.1 The lossless Euler-Bernoulli stiff string equation

Consider a lossless stiff string, defined over $x \in D = [0, L]$, with L the string length in m. The evolution of the transverse displacement $u(x,t)$ of the string over time $t \in \mathbb{R}^+$ is described by:

$$\partial_t^2 u = c^2 \partial_x^2 u - \kappa^2 \partial_x^4 u \qquad c^2 = \frac{T}{\rho \pi r^2} \qquad \kappa^2 = \frac{EI_0}{\rho \pi r^2} \qquad (1)$$

where ∂_t and ∂_x represent partial time and space derivation, respectively; T is the tension, in N; ρ is the string density, in kg/m³; E is Young's modulus of the string material, in Pa; and $I_0 = \frac{\pi r^4}{4}$

is the area moment of inertia for a string of circular cross-section, with r the string radius in m.

Boundary conditions are assumed to be of the simply supported type:

$$u(0,t) = u(L,t) = 0 \qquad \partial_x^2 u(0,t) = \partial_x^2 u(L,t) = 0 \tag{2}$$

2.2 Characteristic polynomial and energy analysis

Examining the behaviour of (1) with a test function $u(x,t) = e^{st+j\beta x}$, where $s = \sigma + j\omega$ is a complex frequency ($\omega = 2\pi f$) and β a wavenumber, leads to the following characteristic polynomial in s:

$$s^2 + c^2\beta^2 + \kappa^2\beta^4 = 0 \qquad \Rightarrow \qquad \sigma = 0, \quad \omega = \sqrt{c^2\beta^2 + \kappa^2\beta^4} \tag{3}$$

where $\sigma = 0$ implies the absence of exponentially decaying solutions. This is confirmed by an energetic analysis of the space-time domain system; multiplying Equation (1) by $\rho_L \partial_t u$ (where $\rho_L = \rho\pi r^2$), and integrating the result over the length of the string, yields:

$$\frac{dH_u}{dt} = 0 \quad , \quad H_u = \int_0^L \left[\frac{\rho_L}{2}(\partial_t u)^2 + \frac{T}{2}(\partial_x u)^2 + \frac{EI_0}{2}\left(\partial_x^2 u\right)^2 \right] dx \tag{4}$$

The system is indeed strictly energy conserving (lossless).

3   A frequency-domain damping model

The basis of this work is the set of experimental measurements performed on harpsichord strings by Cuesta and Valette [7]. They measured the decay times of the transverse modes of a range of strings, and plotted, for each string, the value of the quality factor $Q(f)$ for each of these modes as a function of frequency. The strings were fixed at both ends on a rigid, non-resonant bench. The resulting graph showed a clear maximum, for all strings, between 1 and 4 kHz, indeed corresponding to the part of the spectrum where the human ear is most sensitive. The calculated value of $Q(\omega)$, with $\omega = 2\pi f$, for each mode, was given by:

$$Q(\omega) = -\frac{\omega}{\sigma} \tag{5}$$

where $\sigma(\omega) = -\frac{\log(10)}{\Delta t}$ is the negative decay constant, in s^{-1}, with $\Delta t(\omega)$ the 10 dB decay time of each mode, in s.

Four different damping mechanisms were then examined, two of them found to be non-negligible: air viscosity (prevalent at low frequencies), and internal friction (including string viscoelasticity, prevailing at higher frequencies; heat transport; and dislocations in the string material). The combination of losses due to these four processes provided a very good fit to the experimental data points. Damping due to heat transport and dislocations were found to be indistinguishable from each other in the measured data, and the frequency-independent losses from dislocations showed to be as good a fit as the frequency-dependent losses from heat transport; the former was used in the subsequent theoretical study for the sake of simplicity.

An important and extremely useful aspect of Cuesta and Valette's study is that it provides an expression for $Q(\omega)$ as a function of available physical parameters, that fits the measured data. This is of prime interest for the design and implementation of string physical models, as it

Table 1: Physical parameters used in this work, for a cello D string vibrating in the air.

Symbol	Parameter	Value	Units	Symbol	Parameter	Value	Units
ρ	String material density	$5,535$	kg/m^3	r	String radius	4.55×10^{-4}	m
ρ_a	Air density	1.225	kg/m^3	T	String tension	147.7	N
μ_a	Air kinematic viscosity	1.619×10^{-5}	m^2/s	E	Young's modulus	2.5×10^{10}	Pa

eliminates the need to resort to empirical (and hardly realistic) loss coefficients and processes. The quality factor $Q(\omega)$ as a function of frequency is given by [7]:

$$Q^{-1} = Q_{\text{air}}^{-1} + Q_{\text{visc}}^{-1} + Q_{\text{disl}}^{-1} \tag{6}$$

where $Q_{\text{air}}(\omega)$ is the quality factor associated with air viscosity, $Q_{\text{visc}}(\omega)$ is associated with string viscoelasticity, and Q_{disl} is associated with the vibration of dislocations in the string material [7, 11, 12]:

$$Q_{\text{air}}^{-1} = \frac{\rho_a}{\rho}\left(\frac{\sqrt{2}}{M} + \frac{1}{2M^2}\right), \quad M = \frac{r}{2}\sqrt{\frac{\omega}{\mu_a}} \qquad Q_{\text{visc}}^{-1} = \frac{0.003 E \rho \pi^2 r^6 \omega^2}{4T^2} \qquad Q_{\text{disl}}^{-1} = \frac{1}{18000}$$

where ρ, r, T and E are defined in Section 2.1; ρ_a is the air density, in kg/m^3; μ_a is the kinematic viscosity of air, in m^2/s.

The theoretical, frequency dependent, experimentally validated decay constant $\sigma_{\text{th}}(\omega)$ is now:

$$\sigma_{\text{th}}(\omega) = d_0 + d_1 \sqrt{\omega} + d_2 \omega + d_3 \omega^3 \tag{7}$$

$$d_0 = -\frac{2\rho_a \mu_a}{\rho r^2} \qquad d_1 = -\frac{2\rho_a}{\rho r}\sqrt{2\mu_a} \qquad d_2 = -\frac{1}{Q_{\text{disl}}} \qquad d_3 = -\frac{0.003 E \rho \pi^2 r^6}{4T^2}$$

In the remainder of this paper, we will be considering a cello D string vibrating in the acoustic field. Table 1 gives physical parameter values for this particular system.

4   Transfer to time domain

4.1 Characteristic equation

Suppose one desires to introduce energy dissipation in the string model presented in Section 2. This is equivalent to introducing a non-zero real part to the complex frequency s. Propose the following characteristic equation:

$$s^2 + c^2\beta^2 + \kappa^2\beta^4 + s\left(F(s) + \beta^2 G(s)\right) = 0 \tag{8}$$

where $F(s)$ and $G(s)$ are positive real functions of s, that is [13]:

$$\Re(s) > 0 \;\Rightarrow\; \Re(F(s)) \geqslant 0 \,, \; \Re(G(s)) \geqslant 0 \qquad \text{and} \qquad \Im(s) = 0 \;\Rightarrow\; \Im(F(s)) = 0 \,, \; \Im(G(s)) = 0 \tag{9}$$

4.2 Condition for passivity

The proposed system must be passive, or dissipative: all solutions for the transverse displacement of the string must be exponentially decaying, that is to say that all solutions of Equation (8) must satisfy $\mathfrak{R}(s) = \sigma \leqslant 0$ at all frequencies and wavenumbers. Let us assume that $\sigma > 0$, and prove that (8) has no such solutions. Dividing (8) by s, and equating the real part to 0, yields:

$$\sigma \underbrace{\left(1 + \frac{\left(c^2\beta^2 + \kappa^2\beta^4\right)}{\sigma^2 + \omega^2}\right)}_{A} + \mathfrak{R}\left(F(s)\right) + \beta^2 \mathfrak{R}\left(G(s)\right) = 0 \tag{10}$$

Since $A > 0$, and by (9), $\mathfrak{R}(F(s)) \geqslant 0$ and $\mathfrak{R}(G(s)) \geqslant 0$, Equation (10) has no solutions. The positive realness condition (9) is therefore sufficient so that all solutions of (8) are decaying.

4.3 Previous models

Candidate functions for $F(s)$ and $G(s)$ must be positive real, and convenient to transfer to a space-time domain system of partial differential equations. Previous linear string modelling works [6, 14] have used:

$$F(s) = b_0, \quad G(s) = b_0', \quad b_0, b_0' \geqslant 0 \quad \Rightarrow \quad s^2 + c^2\beta^2 + \kappa^2\beta^4 + b_0 s + b_0' s\beta^2 = 0 \tag{11}$$

which translate directly into space-time domain as:

$$\partial_t^2 u = c^2 \partial_x^2 u - \kappa^2 \partial_x^4 u - b_0 \partial_t u + b_0' \partial_t \partial_x^2 u \tag{12}$$

The first loss term models frequency-independent damping, constant across the spectrum, while the second term introduces frequency-dependent losses. However, this model requires two difficult to calibrate free parameters.

4.4 Rational functions of s

Propose the following:

$$F(s) = b_0 + \sum_{q=1}^{M} \frac{b_q s}{s + a_q} \qquad G(s) = \sum_{q=1}^{M} \frac{b_q' s}{s + a_q'} \qquad b_0, a_q, b_q, a_q', b_q' > 0 \tag{13}$$

F and G are positive real, rational functions of s, and have the interpretation of impedances of two-element ladder circuit structures of the Foster type [13]. This choice of functions results in a $(2M+2)^{th}$ order characteristic polynomial in s. The equivalent system in space-time domain is:

$$\partial_t^2 u = c^2 \partial_x^2 u - \kappa^2 \partial_x^4 u - b_0 \partial_t u - \sum_{q=1}^{M} b_q \partial_t f_q + \sum_{q=1}^{M} b_q' \partial_t \partial_x^2 g_q \tag{14}$$

$$\partial_t f_q = \partial_t u - a_q f_q, \qquad \partial_t g_q = \partial_t u - a_q' g_q, \qquad q = 1, \ldots, M$$

4.5 Energy analysis

Multiplying Equation (14) by $\rho_L \partial_t u$, and integrating over the length of the string, yields the following energy balance, where the boundary terms vanish under simply supported conditions:

$$\frac{dH}{dt} = \frac{d}{dt}\left(H_u + H_f + H_g\right) = -P_0 - P_f - P_g \tag{15}$$

$$H_u = \int_0^L \left[\frac{\rho_L}{2}(\partial_t u)^2 + \frac{T}{2}(\partial_x u)^2 + \frac{EI_0}{2}\left(\partial_x^2 u\right)^2\right]dx$$

$$H_f = \rho_L \int_0^L \left[\sum_{q=1}^M \frac{b_q a_q}{2}\left(f_q\right)^2\right]dx \qquad H_g = \rho_L \int_0^L \left[\sum_{q=1}^M \frac{b_q' a_q'}{2}\left(\partial_x g_q\right)^2\right]dx$$

$$P_0 = \rho_L b_0 \int_0^L (\partial_t u)^2\,dx \qquad P_f = \rho_L \int_0^L \left[\sum_{q=1}^M b_q\left(\partial_t f_q\right)^2\right]dx \qquad P_g = \rho_L \int_0^L \left[\sum_{q=1}^M b_q'\left(\partial_t \partial_x g_q\right)^2\right]dx$$

Since all terms are non-negative, the energy H is non-increasing, and the system is indeed (non-strictly) dissipative.

5   An expression for $\sigma(\omega)$

5.1 General expression

Expanding $s = \sigma + j\omega$ in (8), using the definitions of F and G given in (13), and examining the imaginary part of the resulting equation, yields the $(4M+1)^{th}$ order polynomial in σ:

$$\prod_{q=1}^M \left(\left(\sigma+a_q\right)^2 + \omega^2\right)\left(\left(\sigma+a_q'\right)^2 + \omega^2\right)\cdot\left[2\sigma + b_0 + \sum_{q=1}^M \left(\frac{b_q\left(\sigma^2+\omega^2+2\sigma a_q\right)}{\left(\sigma+a_q\right)^2+\omega^2} + \frac{\beta^2 b_q'\left(\sigma^2+\omega^2+2\sigma a_q'\right)}{\left(\sigma+a_q'\right)^2+\omega^2}\right)\right] = 0 \tag{16}$$

A root finding algorithm can be directly applied to find all the roots of (16), in terms of ω; however, the lack of a closed-form solution leads to a difficult optimisation problem with regards to a fit of σ to σ_{th}. We therefore seek closed-form approximations, better suited for optimisation.

5.2 Approximating σ

For the study of musical strings, one can safely assume that quality factors are large. Consequently, of all the roots of (16), one will be of interest, that satisfies $Q(\omega)$ large, and so $\frac{-\sigma}{\omega} \ll 1$; all other roots will produce valid, but overdamped solutions to the stiff string equation. Additionally, the form of $F(s)$ and $G(s)$ under the assumption of small losses means that $b_0, b_q, b_q' \ll 1, q = 1,\ldots,M$. Finally, as a_q, a_q' have dimensions of frequency (they correspond to the pole locations for F and G), we can assume $\frac{-\sigma}{a_q}, \frac{-\sigma}{a_q'} \ll 1, q = 1,\ldots,M$. We approximate:

$$\left(\sigma+a_q\right)^2 \approx a_q^2, \quad \left(\sigma+a_q'\right)^2 \approx a_q'^2, \quad q = 1,\ldots,M$$

Furthermore, under the small losses condition, the real part of Equation (8) yields an approximated dispersion relation between angular frequency ω and wavenumber β:

$$\omega^2 \approx c^2\beta^2 + \kappa^2\beta^4 \quad \Rightarrow \quad \beta(\omega) \approx \sqrt{\frac{\sqrt{c^4 + 4\kappa^2\omega^2} - c^2}{2\kappa^2}} \tag{17}$$

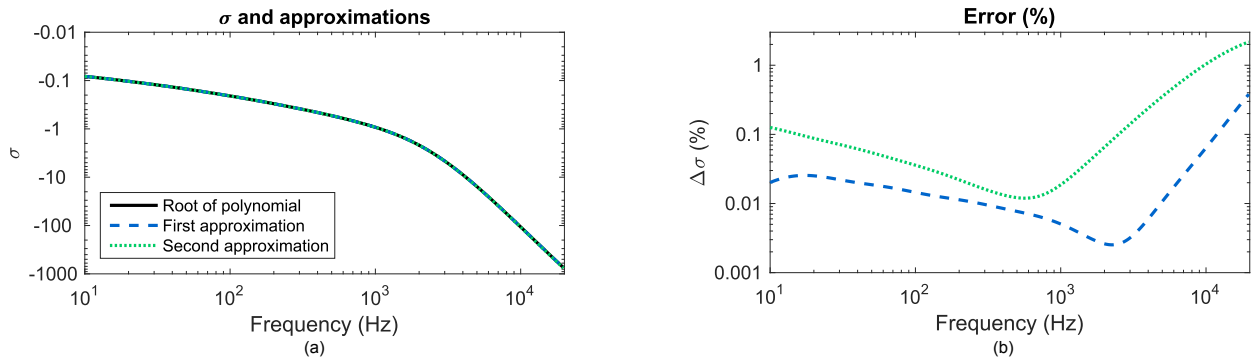which is the same as (3), found in the lossless case. This simply means that damping is

Figure 1: (a) $\sigma(\omega)$ as root of polynomial (16) (solid black line), superposed with approximations (18) and (19) (blue dashed and green dotted lines, resp.) over the frequency range of interest. (b) Error (%) $\Delta\sigma = \left|\frac{\sigma_{\text{root}} - \sigma_{\text{approx}}}{\sigma_{\text{root}}}\right|$ between the polynomial root and approximations (18) and (19) (blue dashed and green dotted lines, resp.).

small enough not to introduce any further inharmonicity than that brought about by the string's bending stiffness. Equation (16) therefore yields a first approximation for $\sigma(\omega)$:

$$\sigma(\omega) \approx -\frac{1}{2}\left(b_0 + \sum_{q=1}^{M}\left(\frac{b_q \omega^2}{a_q{}^2 + \omega^2} + \frac{b_q{}' \beta^2 \omega^2}{a_q{}'^2 + \omega^2}\right)\right)\left(1 + \sum_{q=1}^{M}\left(\frac{b_q a_q}{a_q{}^2 + \omega^2} + \frac{b_q{}' a_q{}' \beta^2}{a_q{}'^2 + \omega^2}\right)\right)^{-1} \quad (18)$$

A further simplification arises for $\sigma(\omega)$, given the previous assumptions and the behaviour of $\beta(\omega)$, assuming that the denominator in (18) is approximately equal to 1:

$$\sigma(\omega) \approx -\frac{1}{2}\left(b_0 + \sum_{q=1}^{M}\left(\frac{b_q \omega^2}{a_q{}^2 + \omega^2} + \frac{b_q{}' \beta^2 \omega^2}{a_q{}'^2 + \omega^2}\right)\right) \quad (19)$$

As a sum of uncoupled terms, the latter approximation is more convenient to approach with a gradient-based optimisation algorithm.

5.3 Validity of approximations

Before proceeding any further, it is helpful to visualise the approximations made in Section 5.2 with respect to the actual value of the root $\sigma(\omega)$ of polynomial (16) that is of interest. To this end, we run a root-finding algorithm on (16) for the cello string described in Section 3, using a set of inferred parameters based on preliminary calculations, and plot the resulting decay constant curve $\sigma(\omega)$ against the two approximated curves from Section 5.2.

As seen in Figure 1, even with both approximations very close to the true polynomial root, the second approximation is clearly inferior to the first one. The error between the polynomial root and the two respective approximations is shown in Figure 1, (b); at most, (18) differs by approximately 0.4% from the root value, whereas the maximal error slightly exceeds 2% for (19). The last step in Section 5.2 is therefore a significant one, and its validity must be verified on final results.

5.4 Optimisation

For a range of N_ω angular frequencies ω_i, corresponding to a 10 Hz — 20 kHz range, we seek to fit our approximation for $\sigma(\omega_i)$ to the theoretical curve $\sigma_{th}(\omega_i)$. As $Q(\omega)$ was the measured quantity in the initial experiment, we optimise $Q = -\frac{\omega}{\sigma}$ instead of σ directly. The least squares method then seeks to minimise the following cost function:

$$E(\boldsymbol{\gamma}) = \sum_{i=1}^{N_\omega} \left(\frac{\omega_i}{\sigma_{th}(\omega_i)} - \frac{\omega_i}{\sigma(\omega_i, \boldsymbol{\gamma})} \right)^2 \tag{20}$$

with $\boldsymbol{\gamma} = [b_0, b_1, \ldots, b_M, b_1{}', \ldots, b_M{}', a_1, \ldots, a_M, a_1{}', \ldots, a_M{}']$ a vector containing the $4M+1$ parameters.

We employ a combination of gradient descent and Newton's method for optimal convergence. Initial guesses are randomised around 0.1 for $b_0, b_q, b_q{}'$, and across the frequency range for $a_q, a_q{}'$. Figure 2 features three optimised curves for $Q(\omega)$, where $\sigma(\omega)$ is approximated to different orders. $M = 2$ already offers a reasonably good fit to the theoretical curve, with a maximal error around 4%; $M = 3$ brings ΔQ under 1%; $M = 4$ brings the maximal error down to 0.2%, at low frequencies.
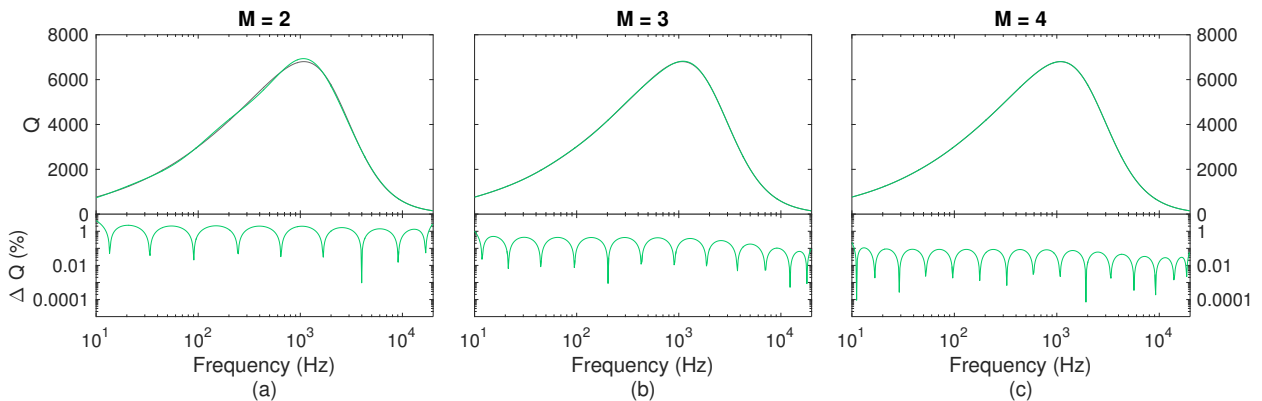

Figure 2: $Q_{th}(\omega)$ (black line), superposed with optimised approximations to various orders (green line), and associated error $\Delta Q = \left| \frac{Q_{th} - Q}{Q} \right|$ (%). (a) $M = 2$; (b) $M = 3$; (c) $M = 4$.

6 Simulations

We can now discretise System (14) into an energy-balanced, dissipative finite difference scheme [15]. Choosing an interleaved, implicit scheme allows for the stability condition to remain unchanged from that of the well-known lossless case [16]. A two-step implicit recurrence can be derived, allowing to compute the state of the string at a given time step using results at the two previous time steps. σ_{th} is first computed from the physical parameters of the string and air; then, the optimisation routine is performed, yielding the appropriate damping coefficients; finally, these coefficients are injected into the scheme, and the recurrence is implemented, calculating the string displacement step by step, at audio sample rates. The string position is initialised with a triangular function whose peak lies at the desired plucking location; the output signal is read out as the displacement of the last moving grid point before the boundary.

Synthetic sound examples are available online[1], for plucked isolated strings, including the cello string used in this paper, as well as a few more musical strings.

7   Discussion

In this paper, we presented a passive model for frequency-dependent losses in linear strings, adaptable to time-domain physical models of musical strings. The loss profile depends directly on the physical parameters of the string and the surrounding air, allowing for realistic damping, tailored to each different string, eliminating the need to rely on heuristic parameters.

This theoretical work still needs quantitative validation; measurements of the same nature that those of Cuesta et al. [7], performed on simulation results, would ensure that the approximations made throughout this work hold until the final modelling steps. If they do, the high reproducibility of simulated results could allow for an exploration of the limits of the original theoretical model.

Another obvious exploration would involve verifying simulation results for different orders of approximation; we saw that for a cello string, $M = 2$ already provided a good fit to the theoretical curve, within a few percent. As M is directly related to computational complexity (which is a major consideration in physical modelling techniques), satisfactory results with a low order of approximation would be undeniably advantageous.

The present model is optimised for the continuous description of linear string vibration; however, simulation and time-domain sound synthesis relies on a discretisation of the system, bringing about further numerical dispersion. To obtain optimal simulated sounds, the damping parameters should be optimised so that this numerical dispersion is taken into account.

Finally, extending this framework to more realistic string modelling could involve nonlinear effects, both in the string itself (geometric nonlinearity) and in the context of collisions with external objects, for excitation (hammers, stoppers, friction) or coupling with parts of the instrument (barriers). Coupling with longitudinal waves was observed in the original experimental paper, which could lead to a full quantitative study and design of a physical model.

Acknowledgements

References

[1] M. Ducceschi and S. Bilbao, "Linear stiff string vibrations in musical acoustics: assessment and comparison of models," *J. Acoust. Soc. Am.*, 2016, under review.

[2] V. Debut, X. Delaune, and J. Antunes, "Identification of the nonlinear excitation force acting on a bowed string using the dynamical responses at remote locations," *Int. J. Mech. Sci.*, vol. 52, no. 11, pp. 1419–1436, 2010.

[3] J. O. Smith III, "Efficient synthesis of stringed musical instruments," in *Proc. Int. Computer Music Conf.*, 1993, pp. 64–71.

---

[1] http://www.charlottedesvages.com/companion/ica-2016

[4] P. M. Ruiz, "A technique for simulating the vibration of strings with a digital computer," Ph.D. dissertation, University of Illinois at Urbana-Champaign, 1970.

[5] A. Chaigne and A. Askenfelt, "Numerical simulations of piano strings. I. A physical model for a struck string using finite difference methods," *J. Acoust. Soc. Am.*, vol. 95, no. 2, pp. 1112–1118, 1994.

[6] J. Bensa, S. Bilbao, R. Kronland-Martinet, and J. O. Smith III, "The simulation of piano string vibration: From physical models to finite difference schemes and digital waveguides," *J. Acoust. Soc. Am.*, vol. 114, no. 2, pp. 1095–1107, 2003.

[7] C. Cuesta and C. Valette, "Evolution temporelle de la vibration des cordes de clavecin," *Acustica*, vol. 66, no. 1, pp. 37–45, 1988.

[8] A. Paté, J.-L. Le Carrou, and B. Fabre, "Predicting the decay time of solid body electric guitar tones," *J. Acoust. Soc. Am.*, vol. 135, no. 5, pp. 3045–3055, 2014.

[9] A. Chaigne and C. Lambourg, "Time-domain simulation of damped impacted plates. i. theory and experiments," *J. Acoust. Soc. Am.*, vol. 109, no. 4, pp. 1422–1432, 2001.

[10] A. Parret-Fréaud, B. Cotté, and A. Chaigne, "Time-domain damping models in structural acoustics using digital filtering," *Mechanical Systems and Signal Processing*, vol. 68, pp. 587–607, 2016.

[11] A. J. Chaigne, "Spectral distribution and damping factors measurements of musical strings using fft techniques," in *Proc. IEEE Int. Conf. Acoustics, Speech, and Signal Processing*, vol. 12, Dallas, USA, 1987, pp. 157–160.

[12] N. H. Fletcher, "Analysis of the design and performance of harpsichords," *Acta Acust. united Ac.*, vol. 37, no. 3, pp. 139–147, 1977.

[13] M. E. Van Valkenburg, *Introduction to modern network synthesis*. Wiley, 1965.

[14] C. Desvages and S. Bilbao, "Two-polarisation physical model of bowed strings with nonlinear contact and friction forces, and application to gesture-based sound synthesis," *Appl. Sci.*, vol. 6, no. 5, p. 135, 2016.

[15] J. C. Strikwerda, *Finite difference schemes and partial differential equations*. Siam, 2004.

[16] S. Bilbao, *Numerical sound synthesis*. Chichester, UK: John Wiley & Sons, Ltd, 2009.